Molecular Crystals and Liquid Crystals
Publication details, including instructions for authors and subscription information:
http://www.tandfonline.com/loi/gmcl18

Solid-State Polymerization of the Unsymmetrically Substituted Diacetylene TS/FBS: Reaction Intermediates and Colour Zones

H.-D. Bauer [a] , A. Materny [a b] , Irene Müller [a] & M. Schwoerer [a]
[a] Physikalisches Institut der Universitat Bayreuth and BIMF, P.O. Box 101251, 0-8580, Bayreuth, Germany
[b] Institut für Physikalische Chemie, Universitat Wurzburg, Marcusstrasze 9-11, D-8700, Wurzburg, Germany
Version of record first published: 04 Oct 2006.

To cite this article: H.-D. Bauer , A. Materny , Irene Müller & M. Schwoerer (1991): Solid-State Polymerization of the Unsymmetrically Substituted Diacetylene TS/FBS: Reaction Intermediates and Colour Zones, Molecular Crystals and Liquid Crystals, 200:1, 205-223

To link to this article: http://dx.doi.org/10.1080/00268949108044242

Mol. Cryst. Liq. Cryst., 1991, Vol. 200, pp. 205–223
Reprints available directly from the publisher
Photocopying permitted by license only

Printed in the United States of America

Solid-State Polymerization of the Unsymmetrically Substituted Diacetylene TS/FBS: Reaction Intermediates and Colour Zones

H.-D. BAUER, A. MATERNY,† IRENE MÜLLER and M. SCHWOERER

Physikalisches Institut der Universität Bayreuth and BIMF, P.O. Box 101251, D-8580 Bayreuth, Germany

(Received October 24, 1990)

We report on absorption and fluorescence of single crystals of the unsymmetrically substituted diacetylene TS/FBS during UV-photopolymerization and thermal polymerization. All the observed reaction intermediates have been identified as diradicals, carbenes and stable oligomers. We compare these results with the well-known diacetylene TS6. The quantum yield of the initiation step as well as the activation energy of the following dark reaction have been determined. Well-separated yellow zones are characteristic for TS/FBS crystals: An additional blue-shifted polymer absorption and a strong fluorescence are typical for these regions. We compare this phenomenon with other chromism effects found with polydiacetylenes and discuss its origin.

Keywords: polydiacetylenes, photochemistry, solid-state polymerization, chromism effects

1. INTRODUCTION

Considerable attention has been paid to diacetylenes during the last years due to their ability to undergo a topochemical solid state polymerization according to

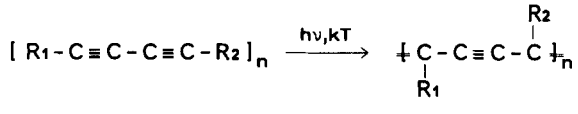

when treated with heat or UV light, respectively.[1,2] After elucidation of the primary reaction steps and intermediate products[3–8] for single crystals of the diacetylene TS6, the main interest was focussed on the π-conjugated polymer molecules and their properties: together with a series of other conjugated materials polydiace-

† Present address: Institut für Physikalische Chemie, Universität Würzburg, Marcusstraße 9–11, D-8700 Würzburg, Germany.

tylenes (PDA's) are candidates for interesting nonlinear properties and, therefore, for future applications in optoelectronics or molecular electronics.[9] The hope to obtain non-centrosymmetric structures which provide nonlinear optical effects or spontaneous polarization brought about the synthesis of unsymmetrically substituted diacetylenes ($R_1 \neq R_2$). In some cases this search for such properties was successful.[10,11]

Though a large number of diacetylenes has been synthesized until today the individual reaction steps have not been object to further investigation since TS6. In this paper we report on the reaction intermediates of a new diacetylene com-

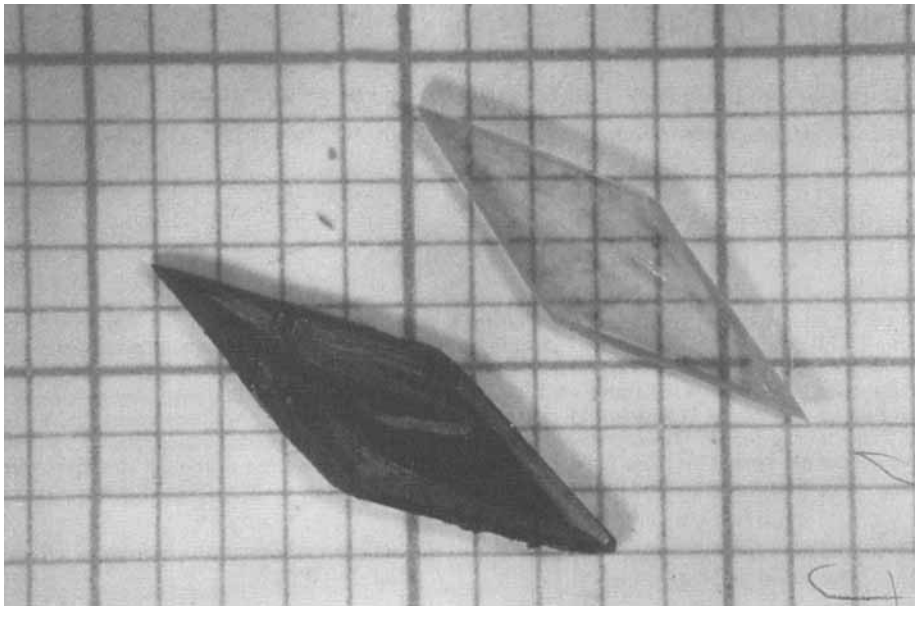

PHOTOGRAPH 1 As-grown TS/FBS single crystals. Left crystal: polymer; right crystal: monomer (low polymer content causes the pink colour). See Color Plate VIII.

TABLE I

Monomer crystal parameters, relative mismatch between monomer and polymer, $\Delta b/b_{Mon}$ (both room temperature values), and time to reach 50% conversion during a thermal polymerization at 60°C, $t_{1/2}$, for TS6, FBS and TS/FBS

Diacetylene/Ref.	TS6[14]	FBS[15]	TS/FBS[12]
a/Å	14.6	13.992	14.400
b/Å	5.15	5.187	5.183
c/Å	15.02	14.091	14.45
β/deg	118.4	114.2	116.5
Δb/b /%	4.66	5.26	5.29
$t_{1/2}$ /h	25	185	70

pound and compare them to the reaction intermediates found in TS6. Furthermore we discuss some interesting properties of the final reaction product, the PDA chain.

2. THE SUBSTANCE

In this paper we mainly report on the unsymmetrically substituted diacetylene TS/FBS with

$$-R_1 = -CH_2-O-SO_2-\bigcirc-CH_3 \quad \text{and} \quad -R_2 = -CH_2-O-SO_2-\bigcirc-F$$

and for comparison—in less detail—on the symmetrically substituted diacetylenes TS6 (both substituents being R_1) and FBS (both substituents being R_2).

TS/FBS was synthesized according to Bertault[12] and Strohriegl.[13] The lozenge-shaped monoclinic crystals were obtained from solution: they are up to 2cm long and some mm thick (Photograph 1). In Table I the crystal parameters and some properties of TS6, FBS and TS/FBS are summarized. TS/FBS and FBS do not show the structural phase transition which occurs for TS6 at 195K.

Often the crystal habit, which is very similar to TS6 and FBS, respectively, is far from perfection: The lozenges provide an unsymmetrically truncated shape. The pink colour of the monomer crystals is due to an initial low polymer content (less than 1%) produced during the crystal growth process, whereas the polymer crystals show a metallic luster (Photograph 1).

On the (100) surface of an as-grown crystal typical zones of different roughness

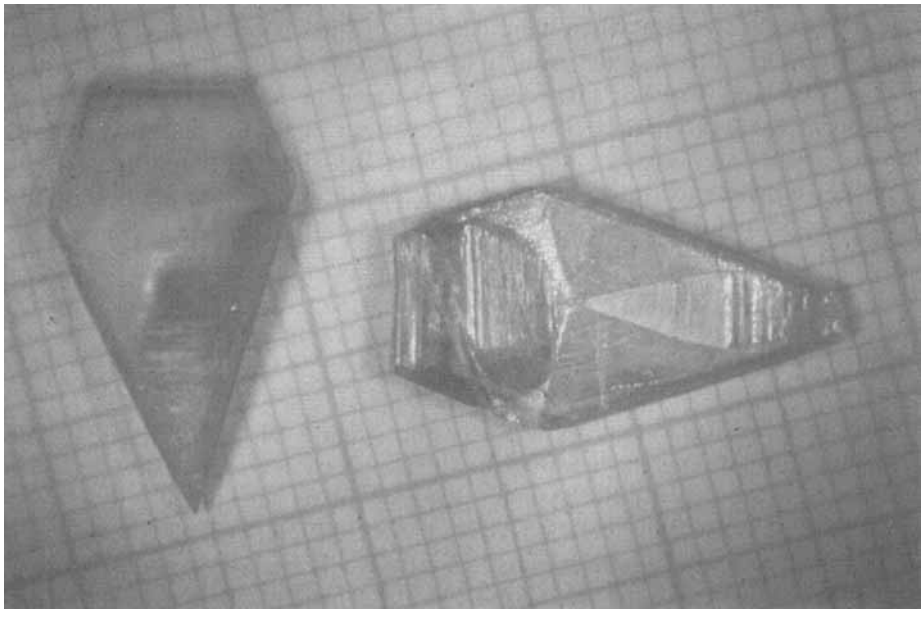

PHOTOGRAPH 2 FBS single crystals showing color zones and corresponding surface "roughness" zones. See Color Plate IX.

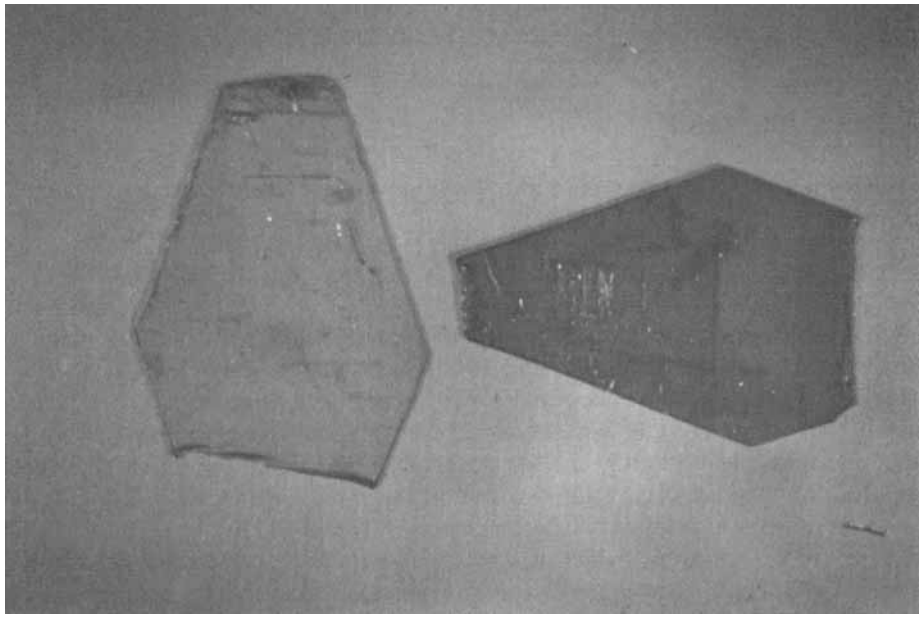

PHOTOGRAPH 3 Platelets, typically 100–200μm thick, cleaved from a FBS single crystal, showing yellow colour zones. Light polarized $\|b$ (crystal on the right) and $\perp b$ (left one), respectively. See Color Plate X.

can be observed, especially when illuminated with light of grazing incidence (Photograph 2). These surface zones usually correspond to yellow regions in the bulk crystal of FBS and TS/FBS, respectively. This can be seen from thin platelets cleaved from the same parent crystal. These colour zones are sharply separated from one another and usually resemble a "butterfly" shape (Photograph 3).

In former growth experiments too rapidly grown crystals showed a by far more imperfect shape and diffuse yellow streaks not localized in certain regions.

3. EXPERIMENTAL

The absorption measurements were performed using a BECKMAN ACTA VII UV/VIS spectrophotometer, modified to fit our special requirements. Luminescence was measured in a polychromatic experiment by an optical multichannel analyzer (B & M OSA 500/PROXITRONIC). An OXFORD CF 1204 optical cryo system was incorporated in both set-ups. An intra-cavity frequency-doubled SPECTRA 2020 argon laser (257nm), a LICONIX NB 4240 helium-cadmium laser (325nm) and a LAMBDA PHYSIK EMG 500 excimer laser (308nm) served as light sources for photopolymerization and fluorescence excitation.

4. RESULTS

4.1 Absorption Spectra of TS/FBS

4.1.1. Monomer crystals. Figures 1 and 2 show the absorption of a monomer crystal at room temperature and at liquid helium temperature. The light was polarized parallel to the *b* axis, i.e. parallel to the preformed polymer chains, which cause the strong absorption band at 590nm (*P*-band) together with a well resolved vibronic structure. In the near UV region the monomer absorption can be seen, too. In Figure 1 a "normal" pink crystal was used, whereas the spectra in Figure 2 are taken from a yellow region under the same conditions as for Figure 1. These spectra show a strong blueshifted absorption at 480nm in addition to the polymer band (henceforth denoted as *Y* band). The vibronic structure is very similar to the one of the *P*-absorption: C—C, C=C and C≡C stretching modes can be identified. If the analyzing light is polarized perpendicular to the polymer chain direction *b*, both bands nearly vanish. Figure 3 shows the variation of the 0-0 peak position of both bands with temperature: Both bands show the same behaviour and thus resemble the early results of Bloor and Hersel[16,17] found with TS6.

Due to the linear π-electron system of the polymer chains partially polymerized diacetylene crystals usually are highly dichroic. The yellow zones also show this strong dichroism, but to a slightly smaller degree: The yellow colour still remains visible when observed with light polarized perpendicularly to the chain direction *b* (see Photograph 2).

4.1.2. Photopolymerization. When irradiated at room temperature with 325nm

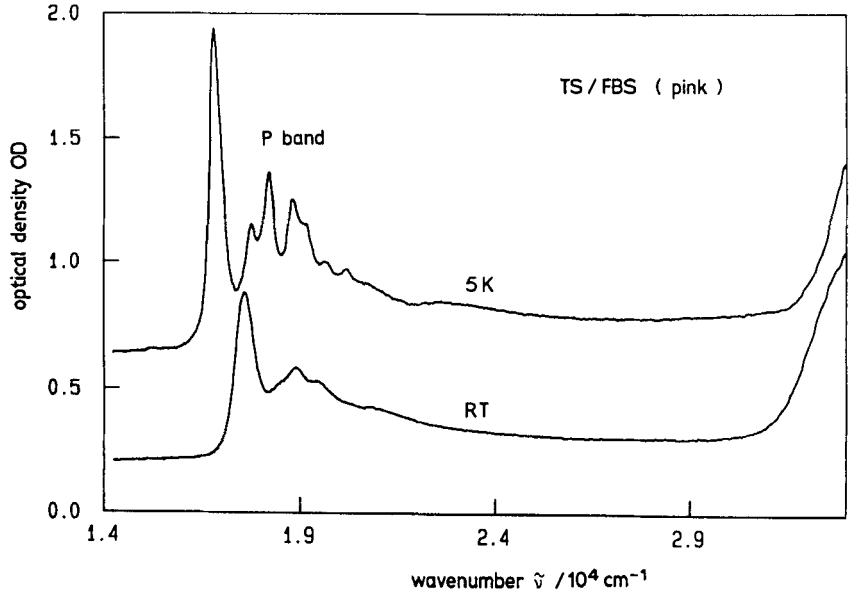

FIGURE 1 Absorption spectra of a pink-coloured TS/FBS sample, 130μm thick, at 5K (upper) and room temperature (lower); polarization ||*b*.

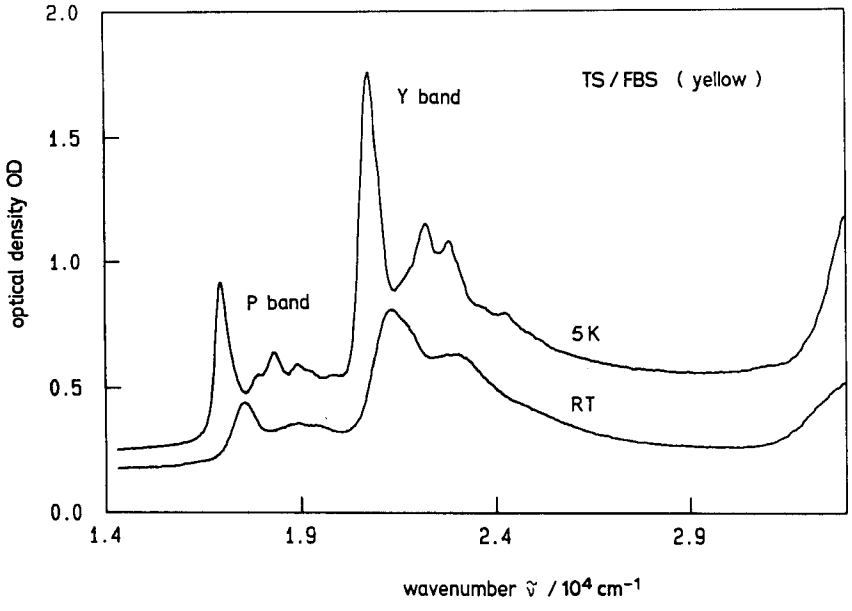

FIGURE 2 Absorption spectra of a yellow color zone of a TS/FBS platelet at 5K (upper) and room temperature (lower); polarization $\|b$.

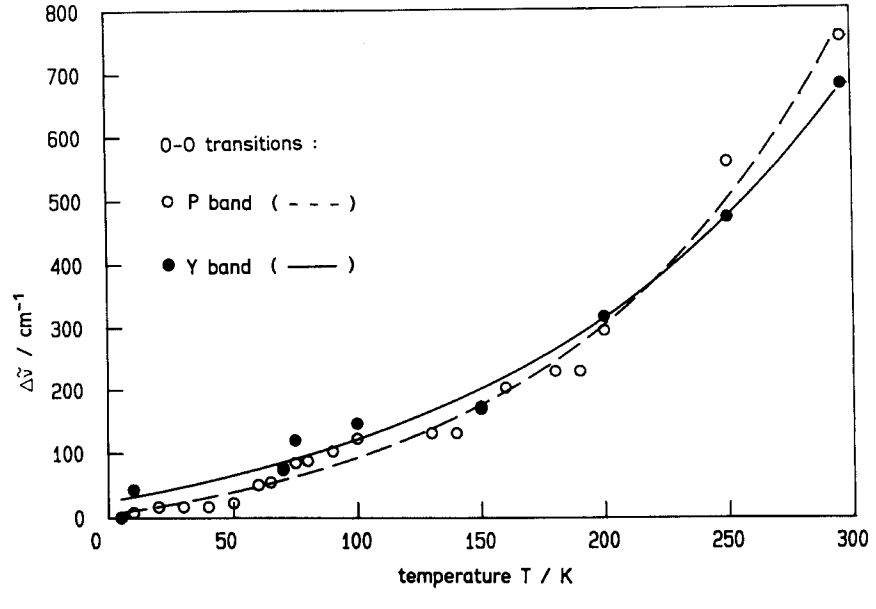

FIGURE 3 Variation of the 0-0 peak position for the polymer absorption (open circles and dashed line) and for the *Y*-band (full circles and solid line).

UV light (0.4mW/mm^2) the monomer platelets show a steplike increase in absorption within the first two minutes, especially in the *P*-absorption region. Later on the increase in absorption is much slower and approximately linear (Figure 4).

At low temperatures the primary photoproduct DR_2 is created: Figure 5 shows the absorption at 5K before and after an excimer laser pulse (15ns, 308nm, 33μJ/mm^2). The vibronic structure is very similar to that of the dimer diradical, DR_2, found as primary reaction product in TS6.[17,18]

We determined the quantum yield of this initiation step to be rather high: 0.4 dimers per UV photon absorbed.

The intermediate products are stable at temperatures below 80K. At 100K the DR_2 undergoes further reaction, yielding a series of reaction intermediates which, in analogy to TS6, can be identified as the DR_n series[4,17] (Figure 6). Further annealing yields an absorption according to the long chain carbenes observed in TS6[4].

The activation energy E_a of chain growth can be determined by an Arrhenius plot of the rate constant $k(T)$ for the growth of the intensity $I(t, T)$ (Figure 7),

$$I(t, T) = I_0 \exp(-k(T)*t)$$

$$k(T) = k_0 \exp(-E_a/(k_B*T))$$

As a result we get for the reaction intermediate DR_2 (Figure 7):

$$E_a = (0.16 \pm 0.05)eV, \qquad k_0 = 0.5*10^{6\pm1}s^{-1}$$

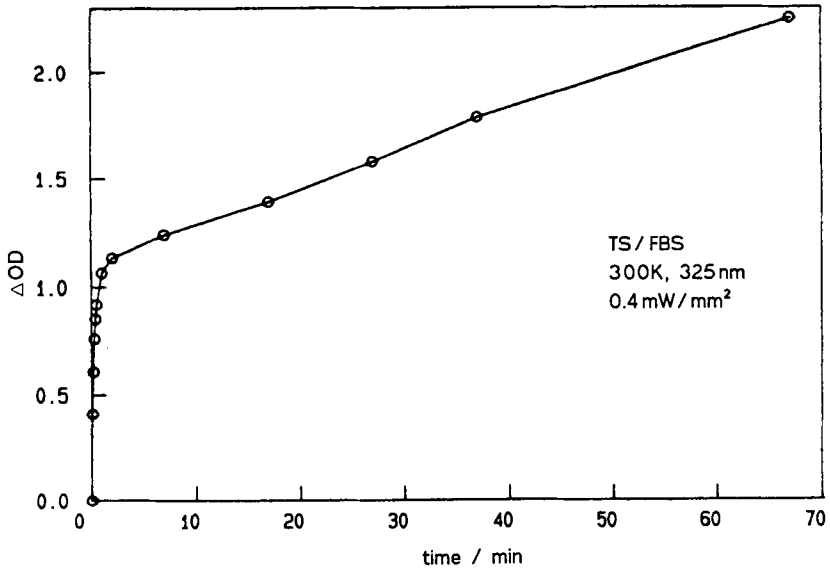

FIGURE 4 Change of optical density at 633nm of a TS/FBS platelet during irradiation with UV light (325nm) of 0.4mW/mm^2 at room temperature. Sample thickness is 140μm. Polarization $\|b$.

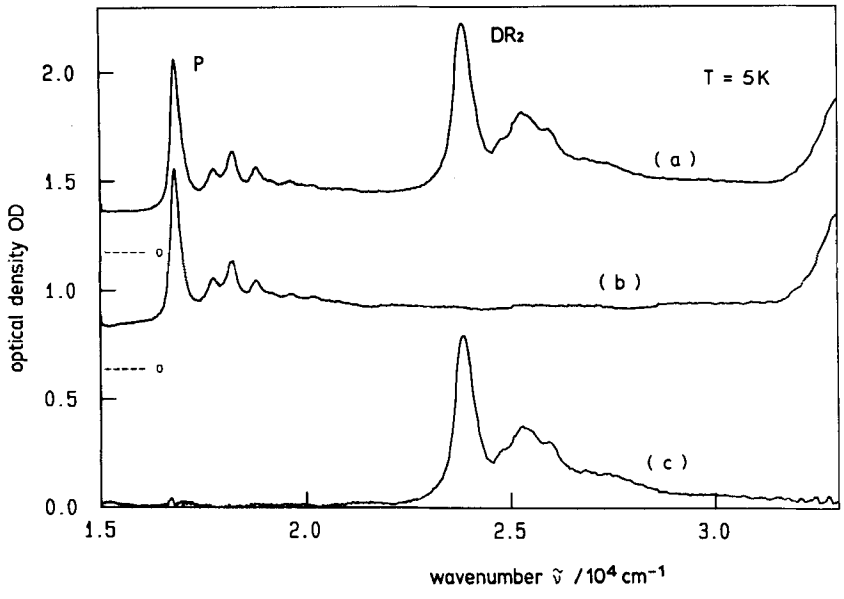

FIGURE 5 Absorption of TS/FBS before (*b*) and after (*a*) UV pulse excitation at 5K. (*c*) = (*a*) − (*b*). The diradical dimer DR_2 is the primary photoproduct for the UV solid state polymerization.

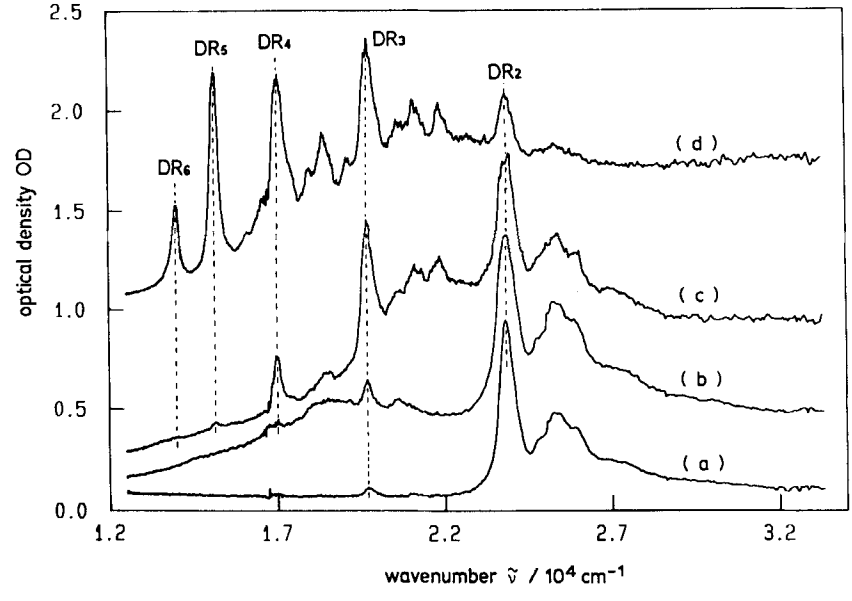

FIGURE 6 Appearance of DR_n reaction intermediates after a single pulse irradiation (308nm) and additional annealing. Annealing temperature and time: (*a*) 5K, 0 min; (*b*) 100K, 6 min; (*c*) 100K, additional 30 min plus 120K, 36 min; (*d*) 130K, 36 min plus 140K, 16 min.

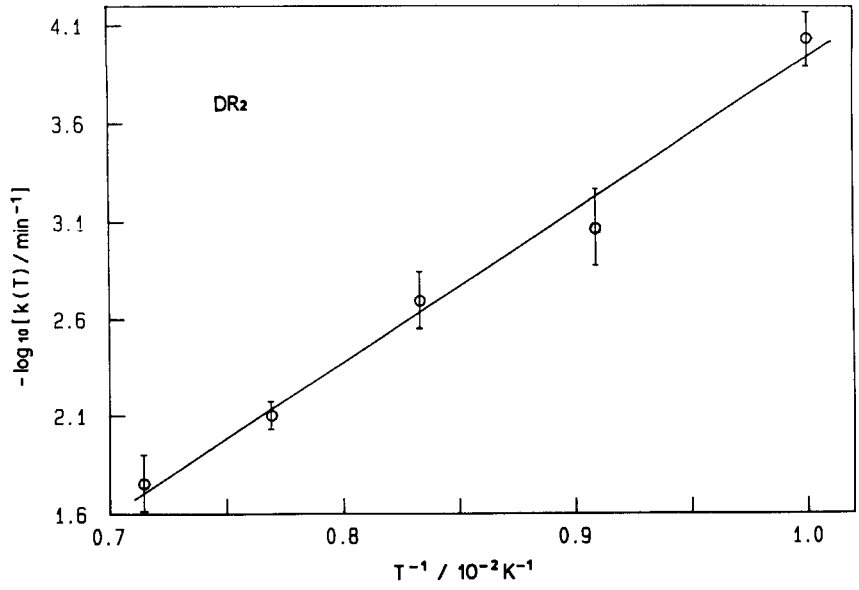

FIGURE 7 Arrhenius plot for determining the activation energy E_a of the chain growth reaction.

This value for E_a is slightly below the one found for TS6[4,18] (0.2 and 0.25 *eV*, respectively).

Again similar to TS6, further irradiation with 325nm UV leads to a series of stable oligomers, SO_n, via chain termination (Sixl in Reference 1). The peak values are nearly the same as in TS6.[17] The successive growth of SO_n absorption bands is shown in Figure 8.

A monomer crystal exposed to 257nm UV radiation also shows the DR_n absorption series and a series of asymmetric carbenes, AC_n (Figure 9). Table II lists the oligomer positions of TS/FBS and TS6 for comparison. They are very similar.

Following Kuhn[19] the extended π-electron system can be described with a simple one-dimensional electron gas model. Exarhos used this theory for polydiacetylenes.[20] For the energy E_n of the 0-0 transition of a polymer chain consisting of n monomer units he gave

$$E_n = h^2/(8ml^2)*(4n + 1) + E_\infty(1 - 1/4n)$$

with

$$l = na_1 + a_2$$

where a_1 is the length of a monomer unit, a_2 stands for the chain ends and m is the electron mass. Varying a_2 and E_∞ yields a good fit of the oligomer absorption series DR_n, AC_n and SO_n. The fit parameters are given in Table III. None of the intermediate absorptions can be identified with the *Y*-absorption shown in Figure 2.

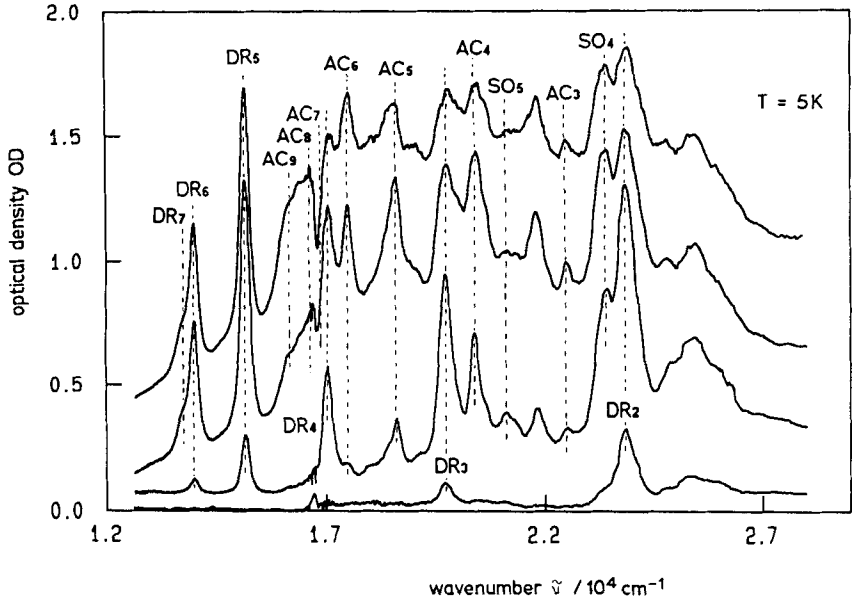

FIGURE 8 Photoproduct series DR_n, AC_n, and SO_n in the course of UV-irradiation with 325nm at 5K after a UV single pulse. Irradiation times and intensities: (*a*) single pulse 308nm, 34μJ/mm², (*b*) 3 min 325nm, (*c*) 61 min, (*d*) 141 min plus 10 min annealing at 250K.

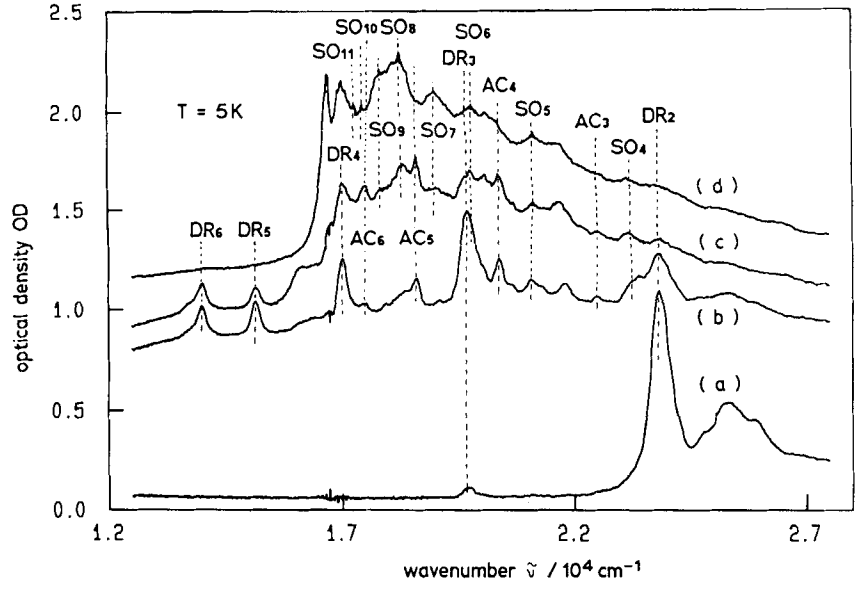

FIGURE 9 Same experiment as in Figure 8, but done with 257nm UV light at 5K. Sample thickness 130μm, UV intensity 0.2mW/mm². Irradiation times: (*a*) 0.4*s*, (*b*) 3*s*, (*c*) 13.5*s*, (*d*) 22.5*s*.

TABLE II

The peak positions of the DR_n, AC_n and SO_n photoproduct series of TS/FBS and TS6, for comparison. The chain length n is given in units of monomers. T = 5K

photoproduct series	chain length n	notation	0-0 transition / cm^{-1} TS/FBS	TS6
diradicals	2	DR_2	23810 ± 20	23731
DRn	3	DR_3	19711 ± 45	19603
	4	DR_4	17036 ± 65	16910
	5	DR_5	15162 ± 65	15067
	6	DR_6	14024 ± 25	14022
	7	DR_7	13921 ± 120	13833
	8	DR_8	14145 ± 130	14181
asymmetric	3	AC_3	22515 ± 40	22524
carbenes	4	AC_4	20420 ± 85	20034
ACn	5	AC_5	18634 ± 60	18468
	6	AC_6	17509 ± 80	17478
	7	AC_7	16925 ± 45	16885
	8	AC_8	16501 ± 60	16536
	9	AC_9	16121 ± 85	16311
	10	AC_{10}	15970 ± 95	16181
stable	4	SO_4	23435 ± 45	23707
oligomers	5	SO_5	21148 ± 55	21385
SOn	6	SO_6	19818 ± 45	19909
	7	SO_7	18978 ± 80	18997
	8	SO_8	18291 ± 40	18371
	9	SO_9	17882 ± 55	17895
	10	SO_{10}	17494 ± 95	17576
	11	SO_{11}	17275 ± 130	17372

TABLE III

Fit parameters for the DR_n, AC_n and SO_n photoproduct series when assuming the Kuhn model

photoproduct series	a_1 / Å	a_2 / Å	E_∞ / cm^{-1}
DRn	5.491	1.792	8265
ACn	5.402	2.377	12048
SOn	5.402	0.520	13573

4.1.3. Thermal polymerization. Figure 10 shows the change in absorption at the wavelengths 590, 480 and 633nm during thermal polymerization at 65°C. Again the samples showed a steplike increase of absorption within the first minutes, especially in the *P*-band. The onset of the autocatalytic reaction regime can be best

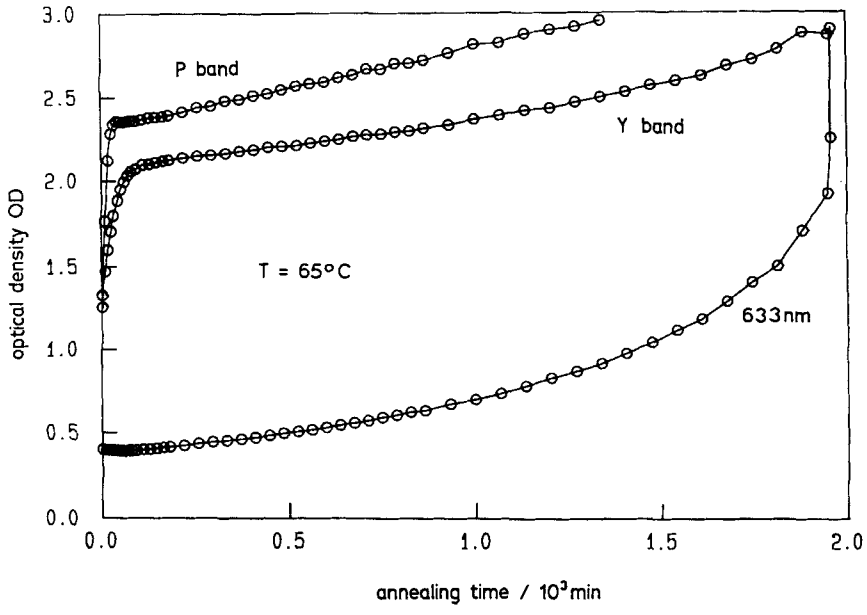

FIGURE 10 Change in optical density of a TS/FBS sample during thermal polymerization at 65°C. Data points for the 0-0 transition of the polymer band (upper), the 0-0 transition of the *Y* band (middle) and at 633nm (HeNe laser, lower).

observed in the 633nm values. The time to reach 50% conversion, $t_{1/2}$, is approximately a factor three longer than for TS6. In addition, a redshift of the polymer absorption appears in the course of the polymerization. This was also found for TS6[21].

4.2. Luminescence Spectra

The striking result for TS/FBS crystals is the fact that their yellow regions show a strong fluorescence (Figure 11), whereas the "normal" pink regions only show a weak one (Figure 12), when excited with light of a wavelength below 480nm and polarized parallel to the *b*-axis. The luminescence has a pronounced vibronic structure, nearly the mirror-image of the absorption. Table IV lists the peak positions of the 0-0 excitation and of the vibrons. The luminescence intensity depends linearly on the excitation intensity. Excitation with light polarized perpendicular to the chain axis results in a small decrease of the "*Y*-emission", whereas the "polymer-emission" vanishes.

5. Discussion

5.1. Reaction intermediates

The polymerization proceeds in the same way as in TS6: Three intermediate product series, diradicals DR_n, dicarbenes DC_n and asymmetric carbenes AC_n can be iden-

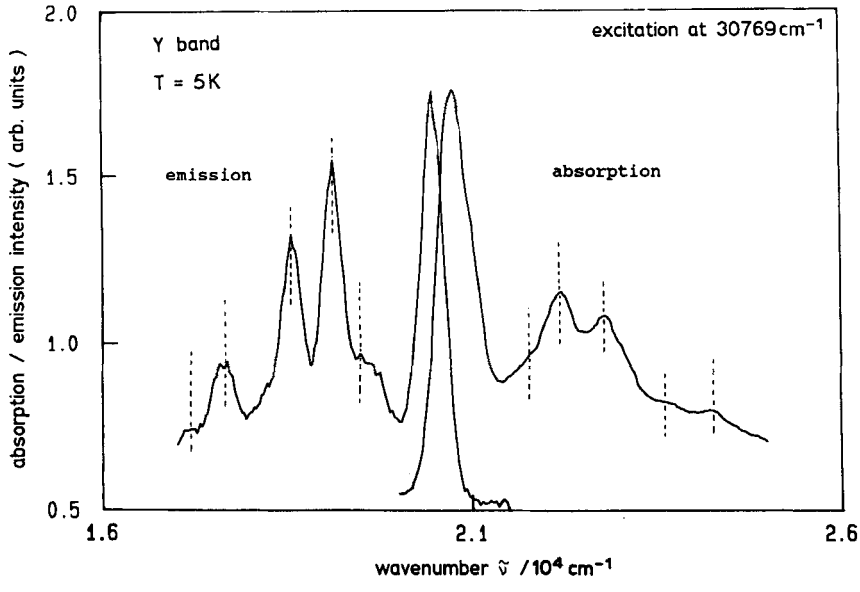

FIGURE 11 Absorption and fluorescence emission spectra of a TS/FBS sample (yellow region). Dashed lines indicate vibronic sidebands of the emission and absorption, respectively.

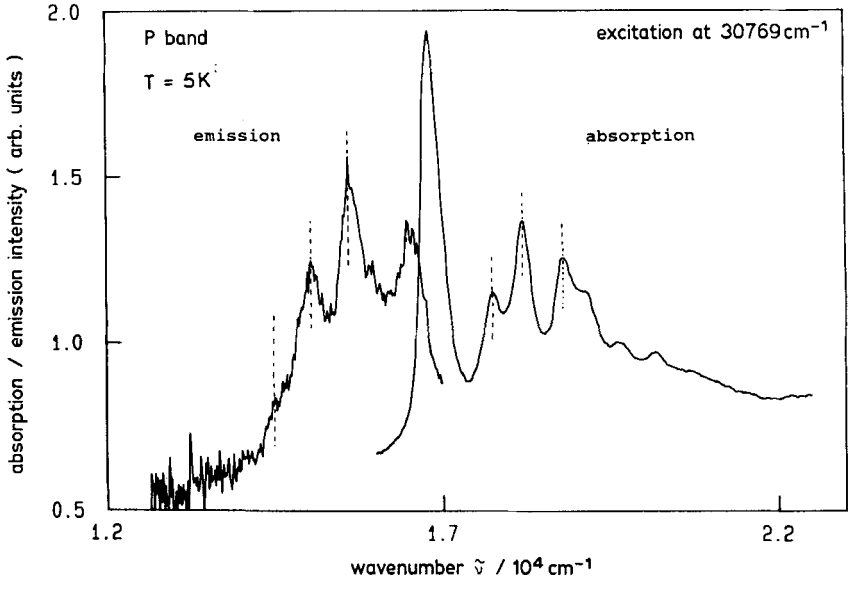

FIGURE 12 Absorption and fluorescence emission spectra of a TS/FBS sample (pink region). Dashed lines indicate vibronic sidebands of the emission and absorption, respectively.

TABLE IV

Peak positions of the 0-0 transition and of the most prominent vibrons for *Y* and *P* band as observed in emission and absorption for TS/FBS

transition	emission / cm^{-1}	absorption / cm^{-1}	difference / cm^{-1}
Y (0-0)	**20337**	**20715**	**378**
vibrons:	- 957	+1012	55
	- 1340	+1415	75
	- 1930	+2064	134
	- 2790	+2870	80
	- 3314	+3543	229
	- 3908	+4204	296
P (0-0)	**16376**	**16828**	**452**
vibrons:	- 965	+ 945	-20
	- 1411	+1397	-14
	- 1995	+1987	- 8

tified. The energetic positions of these intermediates fit the Kuhn electron gas model and are very similar to those of TS6 as is shown in Table II. The change from a butatriene to an acetylene structure could be observed for more than six monomer units. Therefore, there is no significant difference between TS6 and TS/FBS with respect to the polymerization steps.

5.2. Origin of the *Y*-absorption

A common feature of many PDA systems is the presence of drastic chromatic effects: The colour of poly-4BCMU solutions, e.g., depends on the quality of the solvent and on temperature.[22-25]

Although it is still a matter of controversy whether the solvatochromic and thermochromic effects in PDA solutions are a pure single chain phenomenon or aggregation of chains is involved, it seems to be commonly accepted that the major role is played by intermolecular interactions (polymer-solvent or polymer-polymer) which compete with intramolecular interactions (H-bonds between sidegroups of the same polymer chain).[26-28]

Thermochromism was also observed in single crystals of other urethane-substituted PDA's and in thin PDA films.[24,29]

The reason for the strong absorption change first was attributed to a change in the electronic conformation of the chains from an acetylene to a butatriene structure. A number of theoretical calculations, however, proved this assumption not to be correct.[30,31]

The colour shifts can be better explained by thoroughly taking into account the influence of sidegroup packing on the polymer backbone geometry: A packing which favors a planar geometry will provide a π-system of higher conjugation length than a packing which results in a more wormlike or even coiled geometry of smaller conjugation length and, therefore, blueshifted absorption.[32] This idea is strongly supported by Raman measurements.[33]

TABLE V

Polydiacetylenes with differently absorbing chain structures in the crystalline state or in solution. 0-0 transition values in units of cm^{-1}

Name [Ref.]	Side chain group R	partially polym. Crystal planar	nonplanar	Solution planar	nonplanar
TCDU [32]	$-(CH_2)_4-ur-\Phi$	15300 LT	18800 HT	19400	21100
DDU [22]	$-(CH_2)_3-ur-\Phi$	15800		17100	21100
ETCD [27]	$-(CH_2)_4-ur-C_2H_5$	15800	18500		
4BCMU [21]	$-(CH_2)_4-ur-CH_2COO-(CH_2)_3-CH_3$	15800	18500	18900 18700 LT	21500 22000 fi. HT
3BCMU [21]	$-(CH_2)_3-ur-CH_2COO-(CH_2)_3-CH_3$	15700		15900 15800 LT	21300 21000 fi. HT
IPUDO [21]	$-(CH_2)_4-ur-C_3H_7$	15400 LT	18700 HT		
9PA [33]	$-(CH_2)_9OCOCH_2-\Phi$			18700	22200
TS12 [34]	$-(CH_2)_4-SO_3-\Phi-CH_3$		18900		21300
TS6 [35]	$-CH_2-SO_3-\Phi-CH_3$	17500	20500		21500
FBS	$-CH_2-SO_3-\Phi-F$	17800	20700 y.r.		21750
TS/FBS	R_1 = TS6, R_2 = FBS	16800	20700 y.r.		21500

(LT: low temperature phase, HT: high temperature phase, y.r.: yellow region, fi: film, ur: urethane —OCONH—, Φ: phenyl).

Table V summarizes color shifts in a variety of different PDA systems: solutions, crystals, films etc. It is striking how the absorption differences between yellow and pink regions of TS/FBS and FBS crystals fit in this scheme.

From the well structured absorption and the vibronic side bands it seems obvious that long polymer chains are the origin of the *Y* band. The presence of an oligomer of a certain well-defined number of monomer units can be regarded as very unlikely (moreover, the *Y*-absorption could not be identified with a short-chain intermediate

found in our spectroscopic experiments) and short oligomers of different chain length would cause a broadened absorption or even a series of different peaks.

5.3. Origin of the Colour Zones

To clarify the question whether polymerization proceeds homogeneously or nucleation is involved a remarkable number of observations and experiments have been made: Schermann *et al.*[38] found great amounts of edge dislocations in TS6 crystals, revealed by etch pits, which seemed to favour thermal polymerization in their neighbourhood, but not photopolymerization. The observations are consistent with the assumption of two slip systems, (102) [010] and (010) [001]. Using X-ray topography Dudley *et al.*[39] then showed that edge dislocations are preferrably situated in {111} growth sectors and, to a far less extent, in {100} sectors. Young *et al.*[40] determined a dislocation density of $10^{13}m^{-2}$. Small-angle grain boundaries formed by dislocations having a Burgers vector in [010] direction are supposed to force a strain field upon the neighbouring monomer molecules, decreasing their distance from one another and thus increase reactivity considerably, as it is known from pressure studies.[41]

From these facts we conclude that the {111} growth sectors are identical with the observed colour zones and that the polymer chains which give rise to the *Y* absorption are located in close vicinity of the defects mentioned above. The planarity of the chains obviously is disturbed and therefore the conjugation length is decreased. The fact that the *Y* absorption, if present, is usually more intense than the *P* absorption is consistent with the assumption that the activation energy necessary for starting the chain reaction is lowered by the influence of the defects.

Bloor *et al.*[42] also definitely found defect structures and a dependence of crystal habit on growth velocity: The slower a crystal grows, the more the {111} sectors are favoured to grow. A rapid growth process leads to the formation of lozenge-tips showing irregular structures. In Figures 13a–c the growth velocity is assumed to be the same for all facets. As soon as the {111} sectors stop to grow, lozenge-tips are formed which do not contribute to the colour zones (Figure 13d). Figures 13e–h show a case where the growth velocity of the {111} sectors decreases gradually with respect to the other facets. This causes colour zones of more irregular shape as found in most of the crystals.

An incorporation of polymer chains formed during educt synthesis from the solution into the growing {111} sectors via a kind of molecular recognition process seems to be very unlikely because of their length compared to a monomer molecule and because the polymer chains of TS6, FBS and TS/FBS are known to be unsoluble in common organic solvents. Nevertheless, we found that partially polymerized FBS and TS/FBS crystals give solutions of a slightly yellow colour.

5.4. Origin of the Fluorescence

Bloor *et al.*[37] observed fluorescence of TS6 crystals and a rather unstructured absorption in the region of $20500cm^{-1}$ when investigating rapidly grown crystals. This absorption was also seen by Eichele *et al.*[43] and could be attributed to local macroscopic defects. Both, Bloor and Eichele suggested reactive triplet species trapped at crystal defects to bring about the *Y* band.

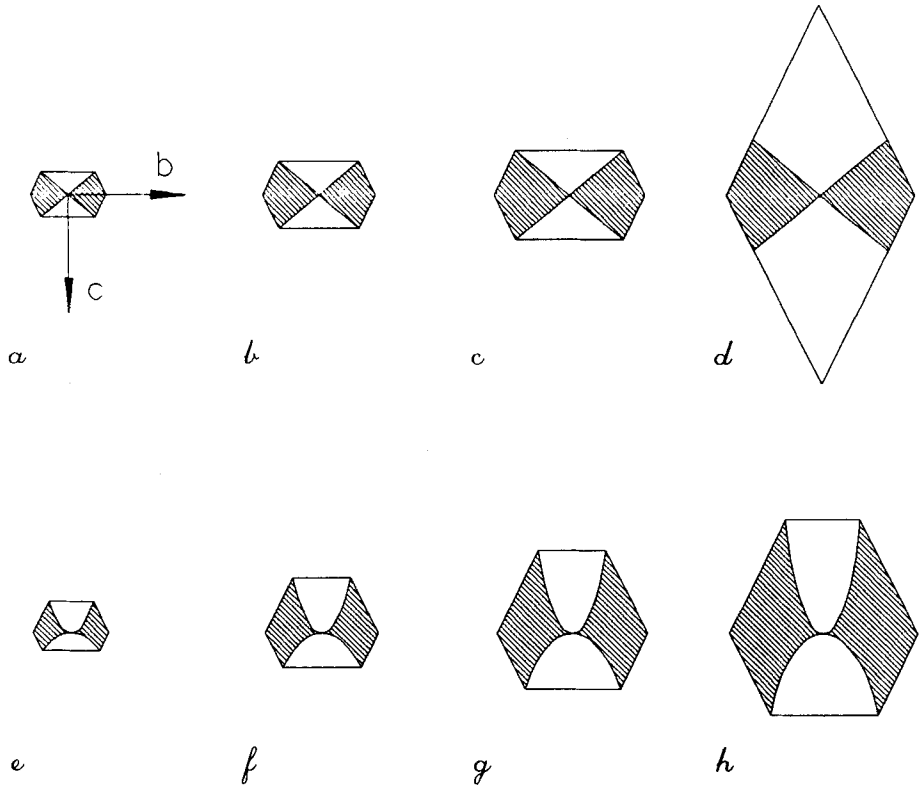

FIGURE 13 Schematic crystal growth scenarios: All facets growing with the same velocity (*a–c*) give straight zone boundaries. A sudden stop in growth of the {111} sectors results in a rather "ideal" habit (*d*). The observed irregular shape of the colour zones results from a variation of growth velocities with respect to one another (*e–h*).

In our experiments we showed the coincidence of the colour zones, the *Y* band, and a strong fluorescence. These three phenomena seem to be "triggered" by the presence of defects, too. The appearance of fluorescence from disturbed PDA chains has been observed in PDA solutions by Brown *et al.*[32] They used a "two-chromophore-model" for interpreting their experiments: disturbed ("coiled") chain segments of low conjugation length acting as blue-shifted absorbers and fluorescence emitters as well as undisturbed ("planar") segments of high conjugation length, which show "normal" absorption and a fluorescence of very low intensity.

Disturbed chains or chain segments deviating from the *b*-direction would also give rise to the observed decrease in polarization ratio (4.1.1. and Photograph 2).

Although some details still have to be checked we think that our observations also can be interpreted in terms of this model.

6. Conclusion

From our observations, previous investigations and from comparison with a great number of very similar chromatic effects in other PDA systems we suggest that

well-defined edge dislocations located preferrably in {111} growth sectors of diacetylene crystals are able to influence the neighbouring monomer units in a way which favours thermal polymerization during the crystal growth process already but results in a non-planar polymer chain structure. This structure carries a distortion of definite character yielding the sharp blueshifted long chain absorption spectrum which we observed. From the difference of the 0-0 peak positions of both absorption bands we conclude this structure to be a coiled more than a wormlike one. For a better understanding of this interesting defect-conformation interaction Raman[44] and CARS experiments[45] are in progress.

Acknowledgement

We thank E. Dormann, T. Vogtmann, W. Lorenz, P. Strohriegl and J. Gmeiner for helpful and stimulating discussions and U. Vollstädt and H. Hereth for technical assistance. This work was supported by the Deutsche Forschungsgemeinschaft (SFB 213/B2) and by the Fonds der Chemischen Industrie.

References

1. H. J. Cantow, editor, *Polydiacetylenes*, Advances in Polymer Science **63** (Springer, Berlin, 1984).
2. D. Bloor and R. R. Chance, editors, *Polydiacetylenes*, NATO ASI Series **E 102** (Nijhoff, The Hague, 1986).
3. M. Schwoerer and H. Niederwald, *Makromol. Chemie Suppl.*, **12**, 61 (1985).
4. H. Niederwald and M. Schwoerer, *Zeitschr. Naturforsch.*, **38a**, 749 (1983).
5. R. Huber, M. Schwoerer, H. Benk and H. Sixl, *Chem. Phys. Lett.*, **78**, 416 (1981).
6. W. Hartl and M. Schwoerer, *Chem. Phys.*, **69**, 443 (1982).
7. H. Gross, H. Sixl, S. F. Fischer and E. W. Knapp, *Chem. Phys.*, **84**, 321 (1984).
8. W. Neumann, H. Sixl, *Mol. Cryst. Liq. Cryst.*, **105**, 41 (1984).
9. J. L. Brédas and R. R. Chance, editors, *Conjugated Polymeric Materials: Opportunities in Electronics, Optoelectronics, and Molecular Electronics*, NATO ASI Series **E 182** (Kluwer, Dordrecht, 1990).
10. E. Dormann, P. Gruner-Bauer and P. Strohriegl, *Makromol. Chem., Makromol. Symp.*, **26**, 141 (1989).
11. P. Strohriegl, J. Gmeiner, I. Müller, P. Gruner-Bauer and E. Dormann, to be submitted to *Ber. Bunsenges. Phys. Chem.*
12. M. Bertault, L. Toupet, J. Canceill and A. Collet, *Makromol. Chem., Rapid Commun.*, **8**, 443 (1987).
13. P. Strohriegl, *Makromol. Chem., Rapid Commun.*, **8**, 437 (1987).
14. D. Bloor, L. Koski, G. C. Stevens, F. H. Preston and D. J. Ando, *J. Mat. Sci.*, **10**, 1678 (1975).
15. J. P. Aimé, M. Schott, M. Bertault and L. Toupet, *Acta Cryst.*, **B 44**, 617 (1988).
16. D. Bloor and C. L. Hubble, *Chem. Phys. Lett.*, **56**, 89 (1978).
17. W. Hersel, PhD thesis, Stuttgart (1981).
18. H. Groß and H. Sixl, *Chem. Phys. Lett.*, **91**, 262 (1982).
19. H. Kuhn, *J. Chem. Phys.*, **17**, 1198 (1949).
20. G. J. Exarhos, W. M. Risen Jr. and R. H. Baughman, *J. Am. Chem. Soc.*, **98**, 481 (1976).
21. D. Bloor, R. L. Williams and D. J. Ando, *Chem. Phys. Lett.*, **78**, 67 (1981).
22. G. N. Patel, R. R. Chance and J. D. Witt, *J. Chem. Phys.*, **70**, 4387 (1979).
23. R. R. Chance, G. N. Patel and J. D. Witt, *J. Chem. Phys.*, **71**, 206 (1979).
24. R. R. Chance, *Macromolecules*, **13**, 396 (1980).
25. R. R. Chance, J. M. Sowa, H. Eckhardt and M. Schott, *J. Phys. Chem.*, **90**, 3031 (1986).
26. L. D. Coyne, C. Chang and S. L. Hsu, *Makromol. Chemie*, **188**, 2311 (1987).
27. J.-P. Aime, J.-L. Fave and M. Schott, *Europhys. Lett.*, **1**, 505 (1986).
28. M. Rawiso, J.-P. Aime, J.-L. Fave, M. Schott, M. A. Müller, M. Schmidt, H. Baumgartl and G. Wegner, *J. Physique*, **49**, 861 (1988).
29. R. R. Chance, R. H. Baughman, C. J. Eckhardt and H. Müller, *J. Chem. Phys.*, **67**, 3616 (1977).

30. S. Suhai, *Phys. Rev. B*, **29**, 4570 (1984).
31. H. Eckhardt, D. S. Boudreaux and R. R. Chance, *J. Chem. Phys.*, **85**, 4116 (1986).
32. A. J. Brown, G. Rumbles, D. Phillips and D. Bloor, *Chem. Phys. Lett.*, **151**, 247 (1988).
33. M. Wenzel and G. H. Atkinson, *J. Am. Chem. Soc.*, **111**, 6123 (1989).
34. H. Müller, C. J. Eckhardt, R. R. Chance and R. H. Baughman, *Chem. Phys. Lett.*, **50**, 22 (1977).
35. S. D. D. V. Roughooputh, D. Phillips, D. Bloor and D. J. Ando, *Polymer Commun.*, **25**, 242 (1984).
36. G. Wenz and G. Wegner, *Makromol. Chemie Rapid Commun.*, **3**, 231 (1982).
37. D. Bloor, D. N. Batchelder and F. H. Preston, *Phys. Stat. Sol.*, **a40**, 270 (1977).
38. W. Schermann, G. Wegner, J. O. Williams and J. M. Thomas, *J. Polym. Sci., Polym. Phys. Ed.*, **13**, 753 (1975).
39. M. Dudley, J. N. Sherwood, D. Bloor and D. Ando, *J. Mater. Sci. Lett.*, **1**, 479 (1982).
40. R. J. Young and J. Petermann, *J. Polym. Sci., Polym. Phys. Ed.*, **20**, 961 (1982).
41. F. Braunschweig and H. Bässler, *Chem. Phys. Lett.*, **90**, 41 (1982).
42. D. Bloor, L. Koski and G. C. Stevens, *J. Mater. Sci.*, **10**, 1689 (1975).
43. H. Eichele and M. Schwoerer, *Phys. Stat. Sol.*, **a43**, 465 (1977).
44. A. Materny, M. Schwoerer and W. Kiefer, in *Proceedings of the 12th International Conference on Raman Spectroscopy*, (1990) p. 742.
45. A. Materny and W. Kiefer, to be published.